Angle-Range Estimation in 1-Bit Wideband Nearfield Systems

Shrayan Das[1], Debarati Sen[1], and Emanuele Viterbo[1]

[1]Affiliation not available

December 15, 2024

Abstract

Next-generation communication systems operating in the mm-Wave and sub-THz bands face high path loss, which can be mitigated by ultra-massive antenna arrays. However, high-resolution quantization in these systems is often impractical, leading to a growing interest in low-resolution, particularly 1-bit ADCs. This letter addresses joint angle and range estimation using 1-bit massive uniform linear arrays (ULA) in wideband near-field systems. We propose a MUSIC-based 1-bit joint angle-range estimation algorithm (JARE-MUSIC) over a near-field tapped-delay line channel model, thus, demonstrating that existing MUSIC-based methods can be adapted for effective wideband near-field localization even under extreme quantization.

Angle-Range Estimation in 1-Bit Wideband Nearfield Systems

Shrayan Das, Debarati Sen, Emanuele Viterbo

***Abstract*—Next-generation communication systems operating in the mm-Wave and sub-THz bands face high path loss, which can be mitigated by ultra-massive antenna arrays. However, high-resolution quantization in these systems is often impractical, leading to a growing interest in low-resolution, particularly 1-bit ADCs. This letter addresses joint angle and range estimation using 1-bit massive uniform linear arrays (ULA) in wideband near-field systems. We propose a MUSIC-based 1-bit joint angle-range estimation algorithm (JARE-MUSIC) over a near-field tapped-delay line channel model, thus, demonstrating that existing MUSIC-based methods can be adapted for effective wideband near-field localization even under extreme quantization.**

***Index Terms*—Near-field, Tapped-delay line channel, 1-bit MUSIC, angle-range estimation, massive ULA**

I. Introduction

Millimeter-wave (mm-Wave) and sub-Terahertz (sub-THz) systems operating in the 30 GHz to 300 GHz band suffer high path loss which can be compensated through ultra-massive antenna arrays. While high-resolution quantization is desirable in such large-scale arrays, it often proves impractical due to the high hardware costs and significant power consumption [1]. Consequently, massive multiple-input multiple-output (MIMO) systems utilizing low-resolution analog-to-digital converters (ADC), have garnered substantial research interest in recent years [2], [3], [4]. Notably, 1-bit ADCs, composed of simple comparators that consume minimal circuit power, have been extensively studied in massive MIMO systems [3], [4].

Existing works on 1-bit massive arrays have exclusively focused on far-field scenarios where the wavefronts are assumed to be approximately planar [5], [6]. This assumption, however, breaks down as we move up the frequency spectrum and deploy more antennas at the transceivers [7]. Hence, it becomes imperative that the near-field performance of 1-bit massive arrays be investigated. Furthermore, previous work on 1-bit DoA estimation has mostly been confined to far-field narrowband frequency flat channels [8], [9], [10]. Because quantization is a nonlinear operation on the time-domain signal, extending these results to wideband systems, where the channel is frequency selective, is not straightforward. This work, therefore, addresses the problem of angle and range estimation using 1-bit massive uniform linear arrays (ULA) over a wideband channel. Specifically, we extend the work in [9] to propose a MUSIC-based 1-bit joint angle-range estimation algorithm (JARE-MUSIC) for wideband near-field localization[1]. In summary, our motivations can be outlined as,

- 1-bit ultra-massive antenna arrays are preferred from an implementation perspective.
- Existing works on quantized wideband massive MIMO systems focus mostly on the communication aspects rather than localization.
- DoA estimation using 1-bit massive linear arrays has been limited to narrowband and far-field scenarios.

Specifically, our contributions to this work are as follows,

- A near-field tapped-delay line channel model is developed.
- The angle and range estimation performance of a single carrier 1-bit wideband near-field system over a tapped-delay line channel is studied.
- It is shown that the reconstructed 1-bit JARE-MUSIC based on the arcsine law [8] and the 1-bit MUSIC proposed in [9] can be applied to wideband near-field scenarios for joint angle and range estimation.

II. Near-field Tapped-delay Line Channel Model

Consider a base station (BS) with a $M = 2N+1 \gg 1$ element uniform linear array (ULA) serving a random user with a single antenna over a line-of-sight (LoS) multipath channel where all arriving multipaths are assumed to have undergone *first order reflections*. The system operates under a single-carrier modulation scheme[2] in a wideband mm-Wave/sub-THz channel with carrier frequency f_c, wavelength λ_c, bandwidth B, and sampling period T_s, which implies $\lambda_c = c/f_c$, with c being the velocity of propagation. Let $\tau_{p,n}$ denote the delay of the p-th path to the n-th antenna relative to the central antenna. Then, the received baseband signal at the n-th antenna at time t is

$$x_n(t) = \sum_{p=0}^{P-1} \gamma_p s(t-\tau_{p,n}) \mathrm{e}^{-\mathrm{j}2\pi f_c \tau_{p,n}} + v_n(t) \quad \forall n \in [-N,N] \quad (1)$$

where γ_p are the complex path gains, $v_n(t)$ is the zero-mean additive white Gaussian noise at the n-th antenna and $s(t)$ is the transmitted training signal at time t defined as

$$s(t) = \sum_{i=-\infty}^{\infty} s[i] g(t - iT_s) \quad (2)$$

$s[i] \in \mathbb{C}$ is the i-th training symbol and $g(t)$ is the pulse-shaping filter. For a *near-field channel*, invoking the Fresnel approximation [7], $\tau_{p,n}$ can be expanded as

$$\tau_{p,n} = \frac{r_{p,n}}{c} \approx \frac{r_p}{c}\left(1 - \frac{nd\sin\theta_p}{r_p} + \frac{n^2 d^2 \cos^2\theta_p}{2r_p^2}\right) \quad (3)$$

where $r_p \in [0.62\sqrt{\frac{D^3}{\lambda_c}}, \frac{2D^2}{\lambda_c}]$ is the distance of the p-th scatterer from the center of the array, $r_{p,n}$ denotes the distance of the

Shrayan Das & Emanuele Viterbo are with the Department of Electrical & Computer System Engineering, Monash University, Clayton, Australia (e-mail:{shrayan.das, emanuele.viterbo}@monash.edu), Debarati Sen is with the G. S. Sanyal School of Telecommunications, IIT Kharagpur, India (e-mail:debarati@gssst.iitkgp.ac.in)

[1]In this work, the terms "angle-range estimation" and "near-field localization" have been used synonymously

[2]For 1-bit ADCs in general, single-carrier systems are considered because the orthogonality of OFDM systems cannot be preserved [11], implying that angle-range estimation needs to be performed in the time domain.

p-th scatterer to the n-th antenna, $\theta_p \in [-\pi/2, \pi/2]$ is the corresponding angle-of-arrival, $D \approx N\lambda_c$ is the effective array aperture dictating the Fraunhofer and Fresnel distances of the array, and $d = \frac{\lambda_c}{2}$ is the inter element separation. Notably, the location of the p-th scatterer under such a setting is given by $(r_p\cos(\theta_p), (r_p\sin(\theta_p))$ with $(r_0\cos(\theta_0), (r_0\sin(\theta_0))$ denoting the LoS component. Using (3), (1) can be simplified to

$$x_n(t) = \sum_{p=0}^{P-1} \bar{\gamma}_p \mathrm{e}^{\mathrm{j}2\pi f_c \left(\frac{nd\sin\theta_p}{c} - \frac{n^2d^2\cos^2\theta_p}{2r_pc}\right)} s(t-\tau_{p,n}) + v_n(t) \quad (4)$$

where $\bar{\gamma}_p = \gamma_p \mathrm{e}^{-\mathrm{j}2\pi f_c \frac{r_p}{c}}$ is the equivalent path gain.

Assuming that the sampling period is chosen such that the Nyquist sampling theorem is satisfied, *i.e.* $T_s = \frac{1}{B}$, it may be observed that the maximum delay difference across the receive antenna array $N\lambda_c/c$ is negligible w.r.t to the sampling period T_s when $N/f_cT_s < 1$, or equivalently, $B/f_c < \frac{1}{N}$. This condition is approximately satisfied for mm-Wave/sub-THz systems with massive arrays [7]. Therefore, neglecting the propagation delay across the array itself, *i.e.* $s(t-\tau_{p,n}) \approx s(t-\frac{r_p}{c})$, we formulate the discrete-time tapped delay line channel model for joint angle-range estimation as follows[3]. Ignoring the noise term and sampling the received signal at the symbol rate yields

$$\begin{aligned} x_n[k] &= x_n(kT_s) \\ &= \sum_{p=0}^{P-1}\sum_{i=-\infty}^{\infty} \bar{\gamma}_p \mathrm{e}^{\mathrm{j}2\pi f_c \left(\frac{nd\sin\theta_p}{c} - \frac{n^2d^2\cos^2\theta_p}{2r_pc}\right)} g((k-i)T_s - \frac{r_p}{c}) s[i] \\ &\overset{(a)}{=} \sum_{p=0}^{P-1}\sum_{j=-\infty}^{\infty} \bar{\gamma}_p \mathrm{e}^{\mathrm{j}2\pi f_c \left(\frac{nd\sin\theta_p}{c} - \frac{n^2d^2\cos^2\theta_p}{2r_pc}\right)} g(jT_s - \frac{r_p}{c}) s[k-j] \end{aligned} \quad (5)$$

where $\overset{(a)}{=}$ is due to the change of variable $i = k-j$. $g(t)$ is assumed to be a Nyquist pulse sampled in the main lobe for $\{t \in \mathbb{R} | t \in (-T_s, T_s)\}$. Let J be the number of symbol-spaced samples of the channel impulse response, such that $J = D+1$, where $D \in [0, \lceil \frac{\max(r_p)}{cT_s} \rceil]$ is the number of channel delay taps, and T_s is the duration of the pulse shaping function with $\lceil\cdot\rceil$ being the ceiling function. Then (5) can be approximated as

$$x_n[k] \approx \sum_{p=0}^{P-1}\sum_{j\in J} \bar{\gamma}_p \mathrm{e}^{\mathrm{j}2\pi f_c \left(\frac{nd\sin\theta_p}{c} - \frac{n^2d^2\cos^2\theta_p}{2r_pc}\right)} g(jT_s - \frac{r_p}{c}) s[k-j] \quad (6)$$

Collecting the sampled received signal across all the antennas at time instances of kT_s, we have

$$\mathbf{x}[k] = \mathbf{H}[k]\mathbf{s}[k] + \mathbf{v}[k] \quad (7)$$

where $\mathbf{s}[k] \in \mathbb{C}^{J\times 1}$ is a J-long vector whose j-th element is $s[k-j]$, and $\mathbf{H}[k] \in \mathbb{C}^{(2N+1)\times J}$ is the channel matrix capturing the effects of the near-field array steering vector, pulse shaping function and path gains at the k-th sampling instance, and taking the form [11]

$$\mathbf{H}[k] \triangleq \boldsymbol{A}(\boldsymbol{\theta},\boldsymbol{r})\bar{\boldsymbol{\Gamma}}[k]\boldsymbol{G}(\frac{r}{c}) \quad (8)$$

where $\boldsymbol{A}(\boldsymbol{\theta},\boldsymbol{r}) = [\boldsymbol{a}(\theta_0, r_0), ..., \boldsymbol{a}(\theta_{P-1}, r_{P-1})]$ with

$$\begin{aligned} \boldsymbol{a}(\theta_p, r_p) = [&\mathrm{e}^{-\mathrm{j}2\pi f_c \left(\frac{-Nd\sin\theta_p}{c} - \frac{N^2d^2\cos^2\theta_p}{2r_{0,p}c}\right)}, ..., 1, \\ &..., \mathrm{e}^{-\mathrm{j}2\pi f_c \left(\frac{Nd\sin\theta_p}{c} - \frac{N^2d^2\cos^2\theta_p}{2r_pc}\right)}]^T \end{aligned} \quad (9)$$

[3]Note that when $s(t-\tau_{p,n}) \neq s(t-\frac{r_p}{c})$, the corresponding phenomenon is termed the spatial-wideband effect and is beyond the scope of the present work [11].

being the near-field array steering vector for the p-th path, $\bar{\boldsymbol{\Gamma}}[k] = \mathrm{diag}(\gamma_0[k], .., \gamma_{P-1}[k])$, $\boldsymbol{G}(\frac{r}{c}) = [\mathbf{g}(\frac{r_0}{c}), ...\mathbf{g}(\frac{r_{P-1}}{c})]^T$, and $\mathbf{g}(\frac{r_p}{c}) = [g(T_s - \frac{r_p}{c}), ..., g(JT_s - \frac{r_p}{c})]$ is a J-long row vector of the samples of the pulse shaping function $g(t - \frac{r_p}{c})$. We assume the path gains to be constant across all the delay taps, and hence, their dependence on the tap indices has been suppressed. The number of multipath P, the maximum channel delay spread D, the pulse shaping waveform $g(\cdot)$, and the structure of the array response $\boldsymbol{a}(\cdot)$ are assumed to be known. Note that for $D = 0$, (8) reduces to the classical *narrowband nearfield* model [7]. Lastly, the training sequence $\mathbf{s}$ is assumed to be a circularly shifted Zadoff-Chu (ZC) sequence of length K [11], K being the channel training length.

III. 1-bit Joint Angle-Range Estimation

Let $\mathbf{h}[k] = \mathrm{vec}(\mathbf{H}[k])$ represent a vector of length $(2N+1)J$, which is formed by taking the transpose of each row of the matrix $\mathbf{H}[k]$ and stacking it below the transpose of the preceding row. Then (7) can be equivalently expressed as

$$\begin{aligned} \mathbf{x}[k] &= \big(\mathbf{s}[k] \otimes \mathbf{I}_{2N+1}\big)\mathbf{h}[k] + \mathbf{v}[k] \\ &= \big(\mathbf{s}[k] \otimes \mathbf{I}_{2N+1}\big)\boldsymbol{U}(\boldsymbol{\theta},\boldsymbol{r})\bar{\boldsymbol{\gamma}}[k] + \mathbf{v}[k] = \tilde{\mathbf{h}}[k]\bar{\boldsymbol{\gamma}}[k] + \mathbf{v}[k] \end{aligned} \quad (10)$$

such that $\boldsymbol{U}(\boldsymbol{\theta},\boldsymbol{r}) \in \mathbb{C}^{(2N+1)J\times P}$ is the near-field angle-range steering matrix across all paths and delay taps, whose p-th column is given by $\boldsymbol{a}\big(\theta_p, r_p\big) \circledast \mathbf{g}(\frac{r_p}{c})$, $\tilde{\mathbf{h}}[k] = \big(\mathbf{s}[k] \otimes \mathbf{I}_{2N+1}\big)\boldsymbol{U}(\boldsymbol{\theta},\boldsymbol{r})$, and $\bar{\boldsymbol{\gamma}}[k] = \mathrm{diag}(\bar{\boldsymbol{\Gamma}}[k])$ with $\circledast$ and $\otimes$ being the column-wise and conventional Kronecker products respectively. A time-slotted radio channel between the user equipment and the base-station is presumed such that $\mathbf{H}[k]$ is taken to be constant over each time slot but varies between one slot to the next due to its dependence on the varying path-gains $\bar{\gamma}_p[k]$. For micro or picocellular setups with low mobility, the range and the angle of arrival for each path do not vary significantly and can thus be assumed to be approximately constant over multiple channel snapshots. Subsequently, channel estimates across K consecutive time slots are obtained as $\mathbf{X} = [\mathbf{x}[1], ..., \mathbf{x}[K]]$, where,

$$\mathbf{X} = \tilde{\mathbf{H}}\tilde{\boldsymbol{\Gamma}} + \mathbf{V} \quad (11)$$

with $\tilde{\mathbf{H}} = [\tilde{\mathbf{h}}[1], ..., \tilde{\mathbf{h}}[K]]$, $\tilde{\boldsymbol{\Gamma}} = [\bar{\boldsymbol{\gamma}}[1], ..., \bar{\boldsymbol{\gamma}}[K]]$ and $\mathbf{V}$ being the noise matrix with zero mean and variance σ_v^2.

III-A Reconstructed 1-bit JARE-MUSIC

Following (10), the 1-bit quantized channel estimates for the k-th time slot can be obtained as [9]

$$\mathbf{y}[k] = \mathscr{Q}(\mathbf{x}[k]) \quad (12)$$

where $\mathscr{Q}(\cdot)$ represents the quantization function such that

$$\mathscr{Q}(z) = \frac{1}{\sqrt{2}}(\mathrm{sign}(\mathscr{R}\{z\}) + \mathrm{j}\ \mathrm{sign}(\mathscr{I}\{z\})) \quad (13)$$

$\mathscr{R}\{z\}$ and $\mathscr{I}\{z\}$ denote the real and imaginary parts of z, respectively. Suppressing the sampling instances and recalling the definition of the normalized covariance matrix of the unquantized data $\mathbf{x}$, one has [10]

$$\bar{\boldsymbol{R}}_x = (\boldsymbol{\Omega})^{-1/2}\boldsymbol{R}_x(\boldsymbol{\Omega})^{-1/2} \quad (14)$$

$\boldsymbol{R}_x = E\{\mathbf{x}\mathbf{x}^H\}$ is the unquantized covariance matrix, and $\boldsymbol{\Omega}$ is a diagonal matrix satisfying $[\boldsymbol{\Omega}]_{n,n}$=$[\boldsymbol{R}_x]_{n,n}$, thus implying

that $\bar{\boldsymbol{R}}_x$ is not necessarily a scalar multiple of $\boldsymbol{R}_x$. It has been shown in literature that $\bar{\boldsymbol{R}}_x$ can be reconstructed from the 1-bit covariance matrix using the arc-sine law as follows [9]

$$\bar{\boldsymbol{R}}_x = \text{sine}(\frac{\pi}{2}\boldsymbol{R}_y) \tag{15}$$

$\boldsymbol{R}_y = E\{\mathbf{y}\mathbf{y}^H\}$ is the 1-bit covariance matrix, and the (u,v)-th element of sine($\mathbf{A}$) is given by $[\text{sine}(\mathbf{A})]_{u,v} = \sin(\mathscr{R}\{\mathbf{A}_{u,v}\}) + \mathrm{j}\sin(\mathscr{I}\{\mathbf{A}_{u,v}\})$. In practice, one can estimate $\boldsymbol{R}_y$ from the sample covariance matrix $\hat{\boldsymbol{R}}_y = \frac{1}{K}\mathbf{Y}\mathbf{Y}^H$ where $\mathbf{Y} = [\mathbf{y}[1],...,\mathbf{y}[K]]$ are the K 1-bit channel samples.

We show below that the reconstructed normalized covariance matrix of the quantized channel estimates in (15) can be used for angular-range estimation if the following lemma holds:

Lemma 1: We assume that the scatterers are uncorrelated. Then with $\boldsymbol{R}_x$ and $\bar{\boldsymbol{R}}_x$ as defined in (14), we have $\boldsymbol{R}_x = \rho\bar{\boldsymbol{R}}_x$ where ρ is a scalar.

Proof: We begin from (6) by expressing the unquantized received signal at the n-th antenna at the kT_s-th instance as

$$x_n = \sum_{p=0}^{P-1}\sum_{j\in J}\bar{\gamma}_p\boldsymbol{a}\big(\theta_p,r_p\big)g(jT_s-\frac{r_p}{c})s[k-j]+v[k] \tag{16}$$

Then, following (16), the diagonal entry of $\boldsymbol{\Omega}$ associated with the n-th antenna is given by

$$\begin{aligned}\sigma^2_{x_n} &= [\boldsymbol{R}_x]_{n,n}\\ &= \sum_{p=0}^{P-1}\sum_{j\in J}|\bar{\gamma}_p\boldsymbol{a}\big(\theta_p,r_p\big)g(jT_s-\frac{r_p}{c})s[k-j]|^2+\sigma_v^2 = \rho\end{aligned} \tag{17}$$

where σ_v^2 denotes the noise power. Eq. (17) implies $\boldsymbol{\Omega} = \rho\mathbf{I}_{2N+1}$, which, when substituted in (14), proves the Lemma.

Thus, for uncorrelated scattering, the normalized covariance matrix of $\mathbf{x}$ is a positive scaled version of its corresponding covariance matrix, thereby implying $\bar{\boldsymbol{R}}_x = \frac{1}{\rho}\boldsymbol{R}_x$, where $\bar{\boldsymbol{R}}_x$ and $\boldsymbol{R}_x$ share the same noise subspace [10]. Therefore, in absence of the unquantized covariance matrix $\boldsymbol{R}_x$, the reconstructed normalized covariance matrix $\bar{\boldsymbol{R}}_x$ can be used for angle and range estimation even though ρ is unknown.

Let $\bar{\boldsymbol{R}}_x$ admit the subsequent eigendecomposition

$$\bar{\boldsymbol{R}}_x = \bar{\boldsymbol{U}}_s\bar{\boldsymbol{\Sigma}}_s\bar{\boldsymbol{U}}_s^H + \bar{\boldsymbol{U}}_n\bar{\boldsymbol{\Sigma}}_n\bar{\boldsymbol{U}}_n^H \tag{18}$$

where $\bar{\boldsymbol{U}}_n$ denotes the noise subspace corresponding to the $2N+1-P$ smallest eigenvalues of $\bar{\boldsymbol{R}}_x$. Then, following the near-field MUSIC algorithm [12], the joint angle and range estimates of the scatterers can be obtained by identifying the P highest peaks of the spectrum

$$f_{NF}(\theta,r) = \arg\max_{\theta,r}\frac{1}{\boldsymbol{a}^H\big(\theta,r\big)\bar{\boldsymbol{U}}_n\bar{\boldsymbol{U}}_n^H\boldsymbol{a}\big(\theta,r\big)} \tag{19}$$

This is achieved via a 2D grid search over angles $\theta\in[-\frac{\pi}{2},\frac{\pi}{2}]$ and ranges $r\in[0.62\sqrt{\frac{D^3}{\lambda_c}},\frac{2D^2}{\lambda_c}]$. Since the 2D MUSIC incurs excessive complexity for angle-range estimation of near-field sources[12], we use the reconstructed normalized covariance matrix from (15) in conjunction with the method proposed in [12] to decouple this joint estimation problem to a sequential angle and range estimation problem involving multiple low-complexity 1D searches as follows.

Note that the antidiagonal elements of the reconstructed normalized covariance matrix are given by

$$\begin{aligned}\bar{\boldsymbol{R}}_x[n,2N+2-n] &= \frac{1}{\rho}\boldsymbol{R}_x[n,2N+2-n]\\ &= \frac{1}{\rho}\Bigg[\sum_{p=0}^{P-1}\sum_{j\in J}\bar{\gamma}_p\mathrm{e}^{\mathrm{j}2\pi f_c\left(\frac{(n-N-1)d\sin\theta_p}{c}-\frac{(n-N-1)^2d^2\cos^2\theta_p}{2r_pc}\right)}\\ &\quad g(jT_s-\frac{r_p}{c})s[k-j]\Bigg]\times\\ &\quad\Bigg[\sum_{p=0}^{P-1}\sum_{j\in J}\bar{\gamma}_p^*\mathrm{e}^{-\mathrm{j}2\pi f_c\left(\frac{(N-n+1)d\sin\theta_p}{c}-\frac{(N-n+1)^2d^2\cos^2\theta_p}{2r_pc}\right)}\\ &\quad g^*(jT_s-\frac{r_p}{c})s^*[k-j]\Bigg]+v_{n-N-1}[k]v^*_{N-n+1}[k]\\ &= \frac{1}{\rho}\sum_{p=0}^{P-1}\sum_{j\in J}|\bar{\gamma}_p\boldsymbol{a}\big(\theta_p,r_p\big)g(jT_s-\frac{r_p}{c})s[k-j]|^2\\ &\quad\times\mathrm{e}^{-\mathrm{j}4\pi f_c\left(\frac{(N-n+1)d\sin\theta_p}{c}\right)}+\sigma_v^2\delta_{n,2N+2-n},\quad n=1,...,2N+1\end{aligned} \tag{20}$$

where $\bar{\boldsymbol{R}}_x[u,v]$ denotes the entry in the u-th row and v-th column of $\bar{\boldsymbol{R}}_x$, and $\delta_{u,v}$ is the Kronecker delta function. A vector $\tilde{\boldsymbol{y}}\in\mathbb{C}^{(2N+1)\times1}$ is now constructed, whose n-th entry is given by $\bar{\boldsymbol{R}}_x[n,2N+2-n]$ without the noise variance, *i.e.*,

$$\begin{aligned}\tilde{\boldsymbol{y}} = [&\frac{1}{\rho}\sum_{p=0}^{P-1}\tilde{\rho}_p\mathrm{e}^{-\mathrm{j}4\pi f_c\left(\frac{Nd\sin\theta_p}{c}\right)},\frac{1}{\rho}\sum_{p=0}^{P-1}\tilde{\rho}_p\mathrm{e}^{-\mathrm{j}4\pi f_c\left(\frac{(N-1)d\sin\theta_p}{c}\right)},\\ &...,\frac{1}{\rho}\sum_{p=0}^{P-1}\tilde{\rho}_p\mathrm{e}^{\mathrm{j}4\pi f_c\left(\frac{(N-1)d\sin\theta_p}{c}\right)},\frac{1}{\rho}\sum_{p=0}^{P-1}\tilde{\rho}_p\mathrm{e}^{\mathrm{j}4\pi f_c\left(\frac{Nd\sin\theta_p}{c}\right)}]^T\end{aligned} \tag{21}$$

where $\tilde{\rho}_p = \sum_{j\in J}|\bar{\gamma}_p\boldsymbol{a}\big(\theta_p,r_p\big)g(jT_s-\frac{r_p}{c})s[k-j]|^2$. The entries of $\tilde{\boldsymbol{y}}$ contain the now decoupled angular information, indicating that DoA estimation can be performed independently of range estimation.

Consequently, $\tilde{\boldsymbol{y}}$ is split into L overlapping subvectors each containing $2N+2-L$ entries with the l-th subvector being,

$$\begin{aligned}\tilde{\boldsymbol{y}}_l = [&\frac{1}{\rho}\sum_{p=0}^{P-1}\tilde{\rho}_p\mathrm{e}^{-\mathrm{j}4\pi f_c\left(\frac{(N-l+1)d\sin\theta_p}{c}\right)},\\ &...,\frac{1}{\rho}\sum_{p=0}^{P-1}\tilde{\rho}_p\mathrm{e}^{-\mathrm{j}4\pi f_c\left(\frac{(L-l-N)d\sin\theta_p}{c}\right)}]\end{aligned} \tag{22}$$

which admits the following decomposition

$$\tilde{\boldsymbol{y}}_l = \tilde{\boldsymbol{B}}\tilde{\mathsf{p}}_l \tag{23}$$

such that

$$\tilde{\boldsymbol{B}} = [\tilde{\boldsymbol{b}}(\theta_0),...,\tilde{\boldsymbol{b}}(\theta_{P-1})]\quad\in\mathbb{C}^{(2N+2-L)\times P} \tag{24}$$

$$\tilde{\mathsf{p}}_l = [\frac{\tilde{\rho}_0}{\rho}\mathrm{e}^{\mathrm{j}4\pi f_c\left(\frac{ld\sin\theta_0}{c}\right)},...,\frac{\tilde{\rho}_{P-1}}{\rho}\mathrm{e}^{\mathrm{j}4\pi f_c\left(\frac{ld\sin\theta_{P-1}}{c}\right)}]^T\ \in\mathbb{C}^{P\times1} \tag{25}$$

with

$$\tilde{\boldsymbol{b}}(\theta_p) = [\mathrm{e}^{-\mathrm{j}4\pi f_c\left(\frac{(N+1)d\sin\theta_p}{c}\right)},...,\mathrm{e}^{-\mathrm{j}4\pi f_c\left(\frac{(L-N)d\sin\theta_p}{c}\right)}]^T \tag{26}$$

Averaging over the outer products of the L subvectors with themselves, we have

$$\tilde{\boldsymbol{R}}_{\tilde{\mathrm{y}}} = \frac{1}{L}\sum_{l=1}^{L}\tilde{\boldsymbol{y}}_l\tilde{\boldsymbol{y}}_l^H = \frac{1}{L}\tilde{\boldsymbol{B}}\left(\sum_{l=1}^{L}\tilde{\mathsf{p}}_l\tilde{\mathsf{p}}_l^H\right)\tilde{\boldsymbol{B}}^H = \frac{1}{L}\tilde{\boldsymbol{B}}\tilde{\boldsymbol{R}}_{\tilde{\mathsf{p}}_l}\tilde{\boldsymbol{B}}^H \tag{27}$$

where $\tilde{\boldsymbol{R}}_{\tilde{\mathsf{p}}_l} = \sum_{l=1}^{L}\tilde{\mathsf{p}}_l\tilde{\mathsf{p}}_l^H$. Following (27), the eigendecomposition of $\tilde{\boldsymbol{R}}_{\tilde{\mathrm{y}}}$ yields

$$\tilde{\boldsymbol{R}}_{\tilde{y}} = \tilde{\boldsymbol{U}}_s \tilde{\boldsymbol{\Sigma}}_s \tilde{\boldsymbol{U}}_s^H + \tilde{\boldsymbol{U}}_n \tilde{\boldsymbol{\Sigma}}_n \tilde{\boldsymbol{U}}_n^H \tag{28}$$

where $\tilde{\boldsymbol{U}}_n$ is the noise subspace. Subsequently, the MUSIC algorithm [12] can be used to estimate the P DoAs by identifying the peaks of the reconstructed 1D spectrum,

$$f(\theta) = \frac{1}{\tilde{\boldsymbol{b}}^H(\theta)\tilde{\boldsymbol{U}}_n\tilde{\boldsymbol{U}}_n^H\tilde{\boldsymbol{b}}(\theta)} \tag{29}$$

The estimated DoAs $\{\hat{\theta}_p\}_{p=0}^{P-1}$ can now be used with the near-field MUSIC spectrum defined in (19) to determine the corresponding ranges. This reduces the 2D peak search in (19) to P equivalent 1D searches. Specifically, the range r_p associated with the p-th DoA estimate $\hat{\theta}_p$ is obtained as

$$\hat{r}_p = \arg\max_r \frac{1}{\boldsymbol{a}^H\big(\hat{\theta}_p, r\big)\bar{\boldsymbol{U}}_n\bar{\boldsymbol{U}}_n^H\boldsymbol{a}\big(\hat{\theta}_p, r\big)} \tag{30}$$

III-B 1-bit JARE-MUSIC

Different from the formulation in III-A, the 1-bit covariance matrix $\boldsymbol{R}_y$ can be directly applied to the angle-range estimation problem without further pre-processing as in (15) by leveraging Lemma 1 and the following observation on $\bar{\boldsymbol{R}}_x$ proposed in [9]

$$\bar{\boldsymbol{R}}_x = \frac{1}{\rho}\boldsymbol{R}_x \approx \frac{\pi}{2}\big(\boldsymbol{R}_y - \big(1-\frac{2}{\pi}\big)\mathbf{I}_{2N+1}\big) \tag{31}$$

where ρ is as defined in (17). Equation (31) shows that $\bar{\boldsymbol{R}}_x$ can be approximated by summing a scaled $\boldsymbol{R}_y$ and a scaled identity matrix $\mathbf{I}_{2N+1}$. Accordingly, the 1-bit covariance matrix from (31) is used with the method proposed in the preceding section to perform a low-complexity sequential angle and range estimation in a near-field system.

III-C Complexity

The complexity of the 1-bit JARE-MUSIC is similar to the modified MUSIC algorithm proposed in [12]. The computational cost is mainly due to the construction and eigendecomposition of matrices $\bar{\boldsymbol{R}}_x$ and $\tilde{\boldsymbol{R}}_{\tilde{y}}$ respectively. Consequently, an approximate complexity of the proposed method is given by $\mathrm{O}((2N+1)^2K+(2N+2-L)^2L+(2N+1)^3+(2N+2-L)^3))$.

III-D Identifiability

Similar to its full-resolution counterpart, the 1-bit JARE-MUSIC requires that $\mathrm{rank}(\tilde{\boldsymbol{B}}) = \mathrm{rank}(\tilde{\boldsymbol{R}}_{\tilde{\mathrm{p}}_l}) = P$. The first condition is met when $P < 2N+2-L$. Additionally, since $\tilde{\boldsymbol{R}}_{\tilde{\mathrm{p}}_l}$ is the sum of L rank-one matrices, it becomes a full rank matrix when $L > P$, thus implying that $P < N+1$. Consequently, the maximum number of resolvable paths is at most $P = N = \frac{M-1}{2}$. Furthermore, $\tilde{\boldsymbol{\Gamma}}$ must be a wide and full row rank matrix, *i.e.* $K \geq P$. In practice, $K \gg P$ so that a reliable estimate of the normalized unquantized covariance matrix can be obtained from the 1-bit channel samples. The above conditions are realizable since mm-Wave/sub-THz channels have a coherence time in the order of nanoseconds [2], allowing a large number of channel snapshots to be recorded.

IV. Results & Discussions

This section evaluates the 1-bit and reconstructed JARE-MUSIC vis-a-vis their full-resolution counterparts. Let, $N = 64$, $L = 20$, $B = 250\,\mathrm{MHz}$, $f_c = 140\,\mathrm{GHz}$, and the number of channel taps $D = 10$. A four-path sparse channel is considered where the arriving multipaths are presumed to have the following spectral characteristics - $\theta_p \sim \mathscr{U}(-\pi/2, \pi/2)$ and $r_p \sim \mathscr{U}[0.62\sqrt{\frac{D^3}{\lambda_c}}, \frac{2D^2}{\lambda_c}]$ respectively.

Fig. 1 examines the 1-bit angle, and range estimates' root mean square error (RMSE) for varying numbers of snapshots between $K = 128, 512, \& 1024$. Notably, for moderate to low numbers of snapshots and values of $1/\sigma_v^2$, the reconstructed and 1-bit JARE-MUSIC algorithms exhibit similar performance. However, when the number of snapshots and $1/\sigma_v^2$ are sufficiently large *e.g.*, $1/\sigma_e^2 = 20\,\mathrm{dB}$ and $K = 1024$, the reconstructed JARE-MUSIC, similar to the reconstructed MUSIC in [9] shows slight improvements, thus, suggesting that the error resulting from the limited number of snapshots may outweigh the approximation error in (31).

Fig. 2 depicts the RMSE variation relative to the number of antennas for $1/\sigma_v^2 = -10\,\mathrm{dB},\ 0\,\mathrm{dB},\ 10\,\mathrm{dB}$, with $D = 0$ and $K = 128$. The plots indicate that for a given $1/\sigma_v^2$, the overall performance of the proposed algorithms improves as the number of antennas increases. Notably, although it has been demonstrated that 1-bit massive arrays can achieve super-resolution angle estimation [9], the impact of quantization on range estimation remained unclear. Specifically, when $N \geq 256$, it is observed from Fig. 2 that both the reconstructed and 1-bit JARE-MUSIC can still provide accurate range estimates, within a few centimeters, even under extreme quantization. However, for massive arrays, the approximation in (31) seems to become more pronounced with increased antennas, suggesting that the approximation error dominates the error from limited snapshots. Consequently, a slight performance superiority of the reconstructed JARE-MUSIC is observed over its 1-bit counterpart when the number of antennas is significantly larger than the number of snapshots. Nonetheless, this difference is minimal, and the two algorithms may be considered equivalent for practical purposes. In summary, although increasing the number of snapshots enhances the algorithms' performance up to a certain point, substantial improvements are primarily achieved through the use of larger arrays.

Finally, Fig. 3 analyses the reconstructed and 1-bit JARE-MUSIC's angular and range resolution capabilities. Specifically, we consider two paths with $\theta_1 = 30^\circ, \theta_2 = 30^\circ + \Delta\theta$ and $r_1 = 10\mathrm{m},\ r_2 = 10\mathrm{m} + \Delta r$ where $\Delta\theta \in [0.5^\circ, 5^\circ]$, $\Delta r \in [0.3\mathrm{m}, 3\mathrm{m}]$, and K=128. A path is said to be successfully resolved if $|\hat{\theta}_i - \theta_i| \leq \frac{\Delta\theta}{2}$ and $|\hat{r}_i - r_i| \leq \frac{\Delta r}{2}\ \forall i \in \{1,2\}$ respectively. Interestingly, both algorithms reach full angular and range resolution at nearly identical thresholds under a limited number of snapshots. This implies that the reconstructed and 1-bit JARE-MUSIC tend to have similar performance when the number of snapshots is low. Therefore, the reconstruction step can likely be omitted, allowing angle-range estimation to be performed directly with the 1-bit channel samples. Finally, the comparisons presented in Figs. 1–3 demonstrate that massive arrays with even 1-bit ADCs can effectively perform near-field angle-range estimation with performance close to that of full-resolution systems while offering reduced hardware complexity.

V. Conclusion

This study demonstrates that the covariance matrix of a 1-bit massive ULA can be effectively used for angle and

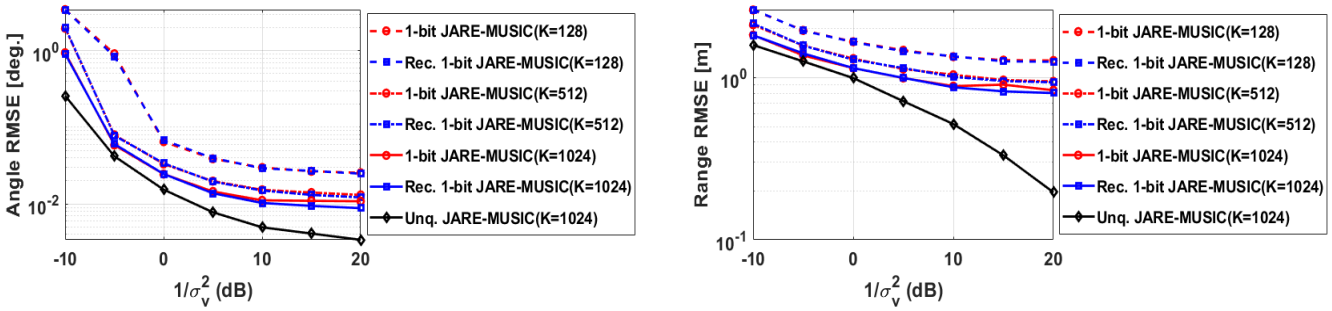

Fig. 1: RMSE of angle & range estimation when number of antennas $M = 2N + 1$=129

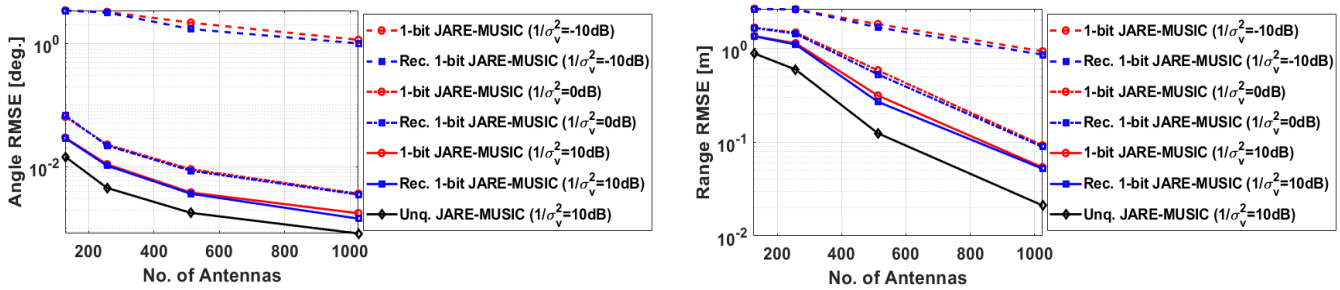

Fig. 2: Variation of RMSE of angle & range estimates with number of antennas when number of snapshots K=128, D=0

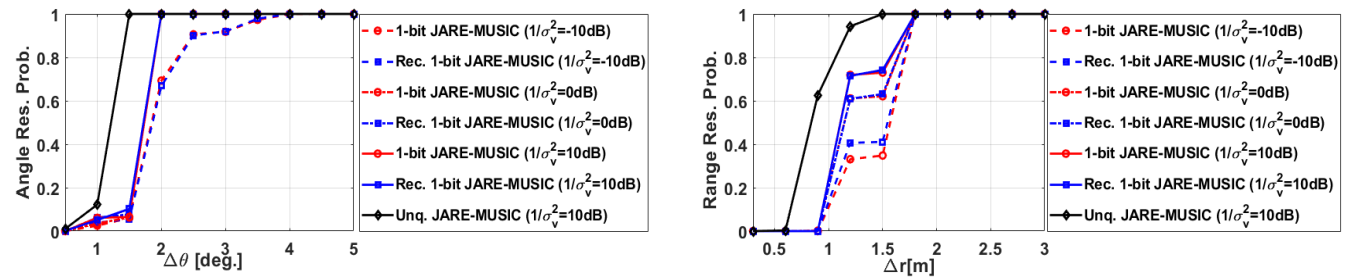

Fig. 3: Resolution probability versus angle & range separation with M=129, K=128, D=0

range estimation in near-field wideband systems. It also finds that the performance of the reconstructed and 1-bit JARE-MUSIC is almost equivalent when the number of snapshots is low, suggesting that the reconstruction step can be skipped, allowing angle-range estimation to be performed directly using the 1-bit channel samples. Additionally, the study concludes that massive arrays with 1-bit ADCs and a sufficient number of antennas can achieve a nearfield performance comparable to full-resolution systems, with only minimal performance degradation.

REFERENCES

[1] A. Li, C. Masouros, A. L. Swindlehurst, and W. Yu, "1-Bit Massive MIMO Transmission: Embracing Interference with Symbol-Level Precoding," *IEEE Commun. Mag.*, vol. 59, no. 5, pp. 121–127, 2021.

[2] T. S. Rappaport, G. R. MacCartney, M. K. Samimi, and S. Sun, "Wideband Millimeter-Wave Propagation Measurements and Channel Models for Future Wireless Communication System Design," *IEEE Trans. Wirel. Commun*, vol. 63, no. 9, pp. 3029–3056, 2015.

[3] C. Mollén, J. Choi, E. G. Larsson, and R. W. Heath, "Uplink Performance of Wideband Massive MIMO With One-Bit ADCs," *IEEE Trans. Wirel. Commun*, vol. 16, no. 1, pp. 87–100, 2017.

[4] S. Rao, A. Mezghani, and A. L. Swindlehurst, "Channel Estimation in One-Bit Massive MIMO Systems: Angular Versus Unstructured Models," *IEEE J. Sel. Areas Commun*, vol. 13, no. 5, pp. 1017–1031, 2019.

[5] X. Chen, L. Huang, H. Zhou, Q. Li, K.-B. Yu, and W. Yu, "One-Bit Digital Beamforming," *IEEE Trans. Aerosp. Electron. Syst*, vol. 59, no. 1, pp. 555–567, 2023.

[6] X. Chen, L. Huang, H. Zhou, Q. Li, and K.-B. Yu, "Performance Analysis of One-Bit Digital Beamforming," *IEEE Trans. Aerosp. Electron. Syst*, vol. 59, no. 6, pp. 8235–8245, 2023.

[7] G. Bacci, L. Sanguinetti, and E. Björnson, "Spherical Wavefronts Improve MU-MIMO Spectral Efficiency When Using Electrically Large Arrays," *IEEE Wireless Communications Letters*, vol. 12, no. 7, pp. 1219–1223, 2023.

[8] O. Bar-Shalom and A. Weiss, "DOA estimation using one-bit quantized measurements," *IEEE Trans. Aerosp. Electron. Syst*, vol. 38, no. 3, pp. 868–884, 2002.

[9] X. Huang and B. Liao, "One-Bit MUSIC," *IEEE Signal Processing Letters*, vol. 26, no. 7, pp. 961–965, 2019.

[10] C.-L. Liu and P. P. Vaidyanathan, "One-bit sparse array DOA estimation," in *2017 IEEE-ICASSP*, pp. 3126–3130, 2017.

[11] I.-S. Kim and J. Choi, "Spatial Wideband Channel Estimation for mmWave Massive MIMO Systems With Hybrid Architectures and Low-Resolution ADCs," *IEEE Trans. Wirel. Commun*, vol. 20, no. 6, pp. 4016–4029, 2021.

[12] J. He, M. N. S. Swamy, and M. O. Ahmad, "Efficient Application of MUSIC Algorithm Under the Coexistence of Far-Field and Near-Field Sources," *IEEE Trans. Signal Process*, vol. 60, no. 4, pp. 2066–2070, 2012.